

# UC Berkeley

## Archaeological X-ray Fluorescence Reports

### Title

SOURCE PROVENANCE OF GILA RIVER QUATERNARY ALLUVIAL OBSIDIAN AND OBSIDIAN ARTIFACT PROVENANCE FROM THE SANCEZ SITE (AZ CC:2:452 ASM), SOUTHEASTERN ARIZONA

### Permalink

<https://escholarship.org/uc/item/7b2987z4>

### Author

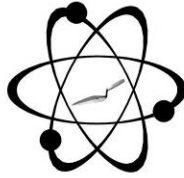
Shackley, M. Steven

### Publication Date

2018-08-09

### Copyright Information

This work is made available under the terms of a Creative Commons Attribution-ShareAlike License, available at <https://creativecommons.org/licenses/by-sa/4.0/>

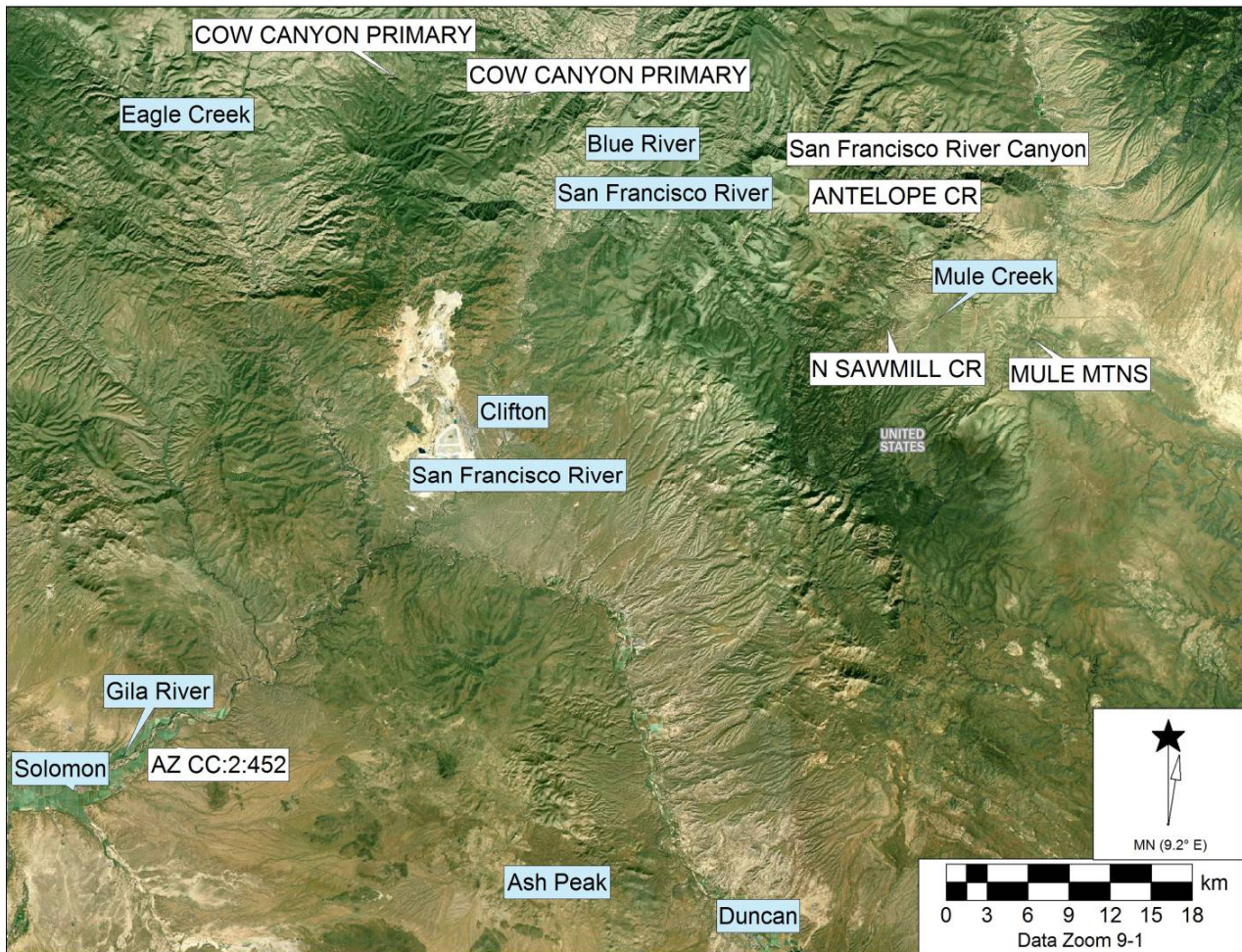


GEOARCHAEOLOGICAL XRF LAB  
A GREEN SOLAR FACILITY

GEOARCHAEOLOGICAL X-RAY FLUORESCENCE SPECTROMETRY LABORATORY  
8100 WYOMING BLVD., SUITE M4-158

ALBUQUERQUE, NM 87113 USA

## SOURCE PROVENANCE OF GILA RIVER QUATERNARY ALLUVIAL OBSIDIAN AND OBSIDIAN ARTIFACT PROVENANCE FROM THE SANCHEZ SITE (AZ CC:2:452 ASM), SOUTHEASTERN ARIZONA



The Sanchez Site (AZ CC:2:452 ASM), primary location of sources of obsidian (in capitals) in the assemblage and relevant features

**SOURCE PROVENANCE OF GILA RIVER QUATERNARY ALLUVIAL OBSIDIAN  
AND OBSIDIAN ARTIFACT PROVENANCE FROM THE SANCEZ SITE (AZ  
CC:2:452 ASM), SOUTHEASTERN ARIZONA**

**DRAFT**

by

M. Steven Shackley, Ph.D., Director  
Geoarchaeological XRF Laboratory  
Albuquerque, New Mexico

Report Prepared for

Professor Robert Hard  
Department of Anthropology  
University of Texas, San Antonio

9 August 2018

## INTRODUCTION

The analysis here of 38 Quaternary alluvial secondary deposit obsidian indicates a diverse source provenance dominated by obsidian from the upstream primary sources of the Cow Canyon Obsidian Complex, and each of the three major localities at the Mule Creek Obsidian Complex in eastern New Mexico, all part of the Mogollon-Datil Volcanic Province (see cover image). All of these sources have been eroding into the Blue, San Francisco, and Gila River systems for over 21 Ma (Shackley 2018; Shackley et al. 2018). The surface and excavated obsidian artifact assemblage (n=16) from the Sanchez Site (AZ CC:2:452 ASM) is generally a reflection of the mix of sources in the Gila River alluvium with slightly less diversity, but still dominated by sources of the Cow Canyon Obsidian Complex.

## ANALYSIS AND INSTRUMENTATION

All archaeological samples are analyzed whole. The results presented here are quantitative in that they are derived from "filtered" intensity values ratioed to the appropriate x-ray continuum regions through a least squares fitting formula rather than plotting the proportions of the net intensities in a ternary system (McCarthy and Schamber 1981; Schamber 1977). Or more essentially, these data through the analysis of international rock standards, allow for inter-instrument comparison with a predictable degree of certainty (Hampel 1984; Shackley 2011a).

All analyses for this study were conducted on a ThermoScientific *Quant'X* EDXRF spectrometer, located at the Geoarchaeological XRF Laboratory, Albuquerque, New Mexico. It is equipped with a thermoelectrically Peltier cooled solid-state Si(Li) X-ray detector, with a 50 kV, 50 W, ultra-high-flux end window bremsstrahlung Rh target X-ray tube and a 76  $\mu\text{m}$  (3 mil) beryllium (Be) window (air cooled), that runs on a power supply operating from 4-50 kV/0.02-1.0 mA at 0.02 increments. The spectrometer is equipped with a 200  $\text{l min}^{-1}$  Edwards vacuum

pump, allowing for the analysis of lower-atomic-weight elements between sodium (Na) and titanium (Ti). Data acquisition is accomplished with a pulse processor and an analogue-to-digital converter. Elemental composition is identified with digital filter background removal, least squares empirical peak deconvolution, gross peak intensities and net peak intensities above background.

### **Trace Element Analysis**

The analysis for mid Zb condition elements Ti-Nb, Pb, Th, the x-ray tube is operated at 30 kV, using a 0.05 mm (medium) Pd primary beam filter in an air path at 100 seconds livetime to generate x-ray intensity  $K\alpha_1$ -line data for elements titanium (Ti), manganese (Mn), iron (as  $Fe_2O_3^T$ ), cobalt (Co), nickel (Ni), copper, (Cu), zinc, (Zn), gallium (Ga), rubidium (Rb), strontium (Sr), yttrium (Y), zirconium (Zr), niobium (Nb), lead (Pb), and thorium (Th). Not all these elements are reported since their values in many volcanic rocks are very low. Trace element intensities were converted to concentration estimates by employing a linear calibration line ratioed to the Compton scatter established for each element from the analysis of international rock standards certified by the National Institute of Standards and Technology (NIST), the US. Geological Survey (USGS), Canadian Centre for Mineral and Energy Technology, and the Centre de Recherches Pétrographiques et Géochimiques in France (Govindaraju 1994). Line fitting is linear (XML) for all elements. When barium (Ba) is analyzed in the High Zb condition, the Rh tube is operated at 50 kV and up to 1.0 mA, ratioed to the bremsstrahlung region (see Davis 2011; Shackley 2011a). Further details concerning the petrological choice of these elements in Southwest obsidians is available in Shackley (1988, 1995, 2005; also Mahood and Stimac 1991; and Hughes and Smith 1993). Nineteen specific pressed powder standards are used for the best fit regression calibration for elements Ti-Nb, Pb, Th, and Ba, and include G-2 (basalt), AGV-2 (andesite), GSP-2 (granodiorite), SY-2 (syenite), BHVO-2 (hawaiite), STM-1 (syenite), QLO-1

(quartz latite), RGM-1 (obsidian), W-2 (diabase), BIR-1 (basalt), SDC-1 (mica schist), TLM-1 (tonalite), SCO-1 (shale), NOD-A-1 and NOD-P-1 (manganese) all US Geological Survey standards, NIST-278 (obsidian), U.S. National Institute of Standards and Technology, BE-N (basalt) from the Centre de Recherches Pétrographiques et Géochimiques in France, and JR-1 and JR-2 (obsidian) from the Geological Survey of Japan (Govindaraju 1994).

The data from the WinTrace software were translated directly into Excel for Windows and into SPSS ver. 21 and JMP 12.0.1 for statistical manipulation. The USGS rhyolite standard RGM-1 is analyzed during each sample run for obsidian artifacts to evaluate machine calibration (Tables 1 through 3). Source assignments were made by reference to source data at <http://swxrflab.net/swobsrsrcs.htm> and Shackley (1995, 2005, 2018; Shackley et al. 2018).

### **The Gila River Quaternary Secondary Deposit Obsidian**

Thirty-eight of the 124 secondary deposit samples (30.6%) were analyzed by EDXRF (Tables 1 and 2 and Figure 1). As discussed below, the distribution of sources from the Cow Canyon Obsidian Complex and the Mule Creek Obsidian Complex is similar to previous studies (Shackley 1992, 2005). The samples were chosen by a grab bag method, reaching into the bag and extracting a sample without looking at the bag. While not a certain representative sample, the more than 30% sample should be near representative.

Table 1. Elemental concentrations and probable source assignments for a sample of 38 Gila River Quaternary alluvium secondary deposit obsidian, and USGS RGM-1 USGS rhyolite standard. All measurements in part per million (ppm).

Sample	Ti	Mn	Fe	Zn	Rb	Sr	Y	Zr	Nb	Ba	Source
2	1233	404	11841	78	248	22	41	120	33	77	Antelope Cr-Mule Cr
8	893	553	9335	77	417	15	73	112	129	0	N Sawmill Cr-Mule Cr
9	1142	431	8540	66	142	86	21	85	16	1132	Cow Canyon
16	1442	503	13118	77	248	29	43	122	28	48	Antelope Cr-Mule Cr
18	1327	561	10929	72	147	109	26	136	14	946	Cow Canyon
20	1384	520	10361	60	145	116	30	141	21	1004	Cow Canyon
21	1424	453	10597	71	124	109	26	132	20	992	Cow Canyon
24	1300	444	9140	58	149	86	23	93	16	1165	Cow Canyon
25	1604	533	12494	78	139	115	20	140	17	989	Cow Canyon
27	1044	563	9927	87	435	10	68	111	123	0	N Sawmill Cr-Mule Cr
28	1080	445	8508	62	137	86	17	85	16	1113	Cow Canyon
33	1245	418	9352	64	144	89	23	95	23	1089	Cow Canyon
36	978	366	10376	64	230	23	40	116	22	67	Antelope Cr-Mule Cr
37	1428	461	10302	52	141	141	23	130	11	1439	Cow Canyon
38	1221	392	8913	52	138	79	22	89	16	1208	Cow Canyon
39	1358	475	10211	56	133	116	21	136	26	1056	Cow Canyon
40	1059	369	8729	49	129	79	21	86	14	1146	Cow Canyon
41	1119	596	10986	95	428	17	73	112	128	0	N Sawmill Cr-Mule Cr
44	1165	463	9086	73	147	89	25	90	20	1173	Cow Canyon
45	1275	489	9879	60	142	113	25	137	18	1019	Cow Canyon
47	1132	445	8815	61	150	88	17	89	18	1162	Cow Canyon
51	954	398	10482	65	250	24	46	115	23	36	Antelope Cr-Mule Cr
55	1208	428	8901	66	143	87	21	91	14	1160	Cow Canyon
57	1306	479	9757	71	152	92	23	93	16	1134	Cow Canyon
60	1248	505	10078	70	143	110	22	134	23	997	Cow Canyon
65	1068	376	10955	95	240	26	41	122	32	44	Antelope Cr-Mule Cr
81	1232	506	10413	61	137	113	23	141	18	1039	Cow Canyon
86	1462	456	10208	67	134	137	18	131	18	1453	Cow Canyon
92	1041	493	9281	69	193	19	29	122	30	37	Mule Mtns-Mule Cr
93	1250	372	11775	80	231	28	38	118	29	90	Antelope Cr-Mule Cr
95	958	369	10303	81	241	21	42	119	28	46	Antelope Cr-Mule Cr
96	1177	430	9588	89	140	113	23	131	17	1021	Cow Canyon
97	1095	425	9015	64	178	15	30	115	32	70	Mule Mtns-Mule Cr
100	1305	420	9610	79	130	83	17	92	12	1087	Cow Canyon
102	1661	623	12898	90	170	91	28	218	28	1088	Cow Canyon
106	1095	428	8827	62	173	15	25	114	28	65	Mule Mtns-Mule Cr
109	1412	527	11053	73	140	85	21	97	20	1047	Cow Canyon
114	1360	457	9798	89	136	129	16	117	15	1404	Cow Canyon
RGM1-S4	1550	308	13119	36	149	109	27	218	14	830	standard
RGM1-	1602	315	13150	45	148	104	24	213	10	831	standard

S4												
----	--	--	--	--	--	--	--	--	--	--	--	--

Table 2. Frequency distribution of the obsidian source provenance from the data in Table 1 (above).

Source	Frequency	Percent
Cow Canyon	25	65.8
Antelope Cr-Mule Cr	7	18.4
Mule Mtns-Mule Cr	3	7.9
N Sawmill Cr-Mule Cr	3	7.9
Total	38	100.0

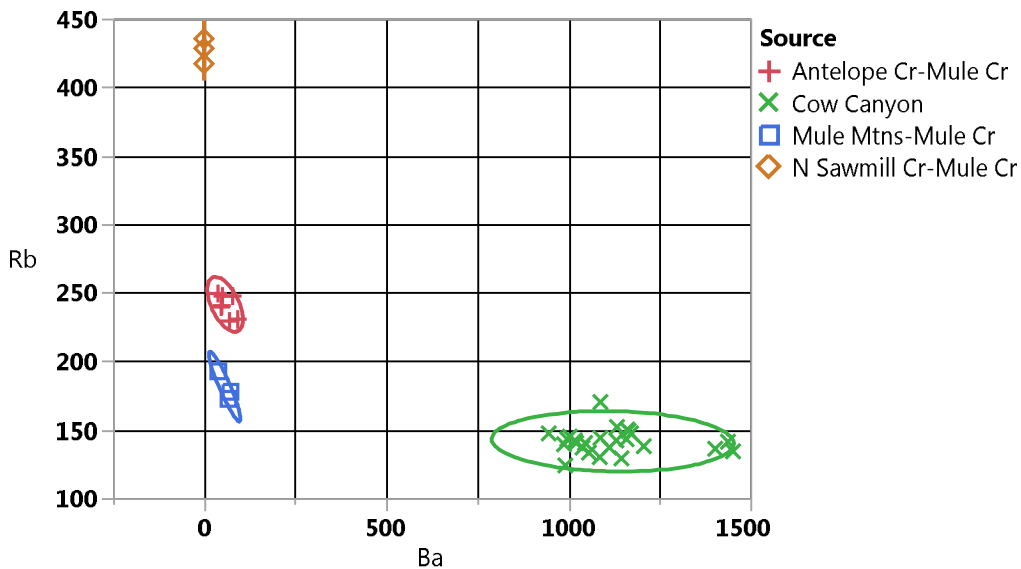


Figure 1. Ba versus Rb bivariate plot of the distribution of secondary deposit obsidian in Gila River Quaternary alluvium . All measurements in parts per million (ppm). Confidence ellipses at 95%. See Tables 1 and 2.

### Discussion

The distribution of sources in the Gila River Quaternary alluvium is not significantly different from results in earlier studies (Shackley 1992, 2005). The primary source localities in the Cow Canyon Obsidian Complex are up river at the headwaters of Eagle Creek, and west of the Blue River in the regolith above Cow Canyon (Shackley 1988, 1995, 2005, 2018). Cow Canyon drains east into the Blue River, on into the San Francisco River and then into the Gila River. It also erodes directly through Eagle Creek into the Gila from the north (Shackley 1992,

2005). During the Plio/Pleistocene when the flow of the ancestral rivers was much greater than today, the sediment load from these sources was so rapid and voluminous that in the lacustrine sediments now called the 111 Ranch Formation nodule sizes are as large as at the Cow Canyon primary sources, about 50 mm in largest diameter (Houser et al. 1985; Shackley 2005).

The Mule Creek sources, particularly Antelope Creek, dated to >19 Ma has been eroding through Antelope and Cienega Creeks directly into San Francisco River canyon, and into the Gila. Today you can see marekanites of Antelope Creek strewn along Cienega Creek all the way to the San Francisco River canyon. Nodule sizes are up to at least 10 cm (100 mm) today. The other two localities at Mule Creek, North Sawmill Creek (ca. 17 Ma) and Mule Mountains (ca. 21 Ma) similarly erodes north into San Francisco River canyon (Shackley et al. 2018). This dominance of Cow Canyon over the Mule Creek sources is typical, partly because Cow Canyon upstream is distributed over a much larger area and secondary deposits drain through multiple channels. The age of Cow Canyon rhyolite is unknown other than certainly Tertiary (Neogene). See the discussion of the Duncan obsidian source below. The Mogollon-Datil obsidian sources have been used throughout prehistory from the Paleoindian through the historic period (Hamilton et al. 2013; Mills et al. 2013; Shackley 2007; Shackley et al. 2018).

### **The Sanchez Site Assemblage**

A sample of 12 obsidian artifacts from the Sanchez Site was analyzed by EDXRF derived from surface and subsurface contexts (Tables 3 and 4 and Figure 2). The sources present are the same as those recovered from the Quaternary alluvium along the Gila River with a greater dominance of Cow Canyon (Tables 3 and 4). All the artifacts including the two Tularosa Corner-notched projectile points produced from Cow Canyon obsidian (see Figure 3) could be produced from secondary deposit obsidian, although likely farther upstream from this locality where the

nodule sizes are somewhat larger. It is also possible that the raw material was procured from the primary sources in the uplands.

Table 3. Elemental concentrations and source assignments for the Sanchez Site obsidian artifacts and USGS RGM-1 rhyolite standard. All measurements in parts per million (ppm).

Sample	Context	Ti	Mn	Fe	Zn	Rb	Sr	Y	Zr	Nb	Ba	Source
120	Surface	1386	465	10233	78	146	136	21	130	19	1412	Cow Canyon
211	Surface	1370	491	9944	69	150	111	22	140	17	967	Cow Canyon
747	Surface	1290	435	9599	68	144	138	26	129	20	1351	Cow Canyon
836	Surface	1265	501	9512	89	139	110	26	132	18	932	Cow Canyon
847	Surface	1293	429	9673	51	127	105	29	136	20	943	Cow Canyon
54	Excavation	1312	414	9411	121	132	134	18	117	18	1308	Cow Canyon
56	Excavation	1237	446	9584	49	142	135	24	128	14	1445	Cow Canyon
60	Excavation	1383	425	9932	67	142	137	20	134	16	1404	Cow Canyon
72	Excavation	1368	723	10555	229	449	14	61	105	95	16	N Sawmill Cr-Mule Cr
78	Excavation	1414	559	11265	92	166	125	25	149	21	905	Cow Canyon
103	Excavation	1002	327	7786	43	112	71	23	83	16	1274	Cow Canyon
182	Excavation	674	170	5277	16	0	10	4	20	1	0	not obsidian
844	Below Sanchez	780	369	9916	58	251	23	41	118	23	0	Antelope Cr-Mule Cr
845A	Below Sanchez	891	403	10402	51	259	23	43	120	32	50	Antelope Cr-Mule Cr
845B	Below Sanchez	940	424	10793	91	261	24	49	116	27	62	Antelope Cr-Mule Cr
846	Below Sanchez	1043	429	8915	76	175	19	25	123	29	50	Mule Mtns-Mule Cr
RGM1-S4		1477	301	13064	44	145	103	26	221	10	845	standard
RGM1-S4		1581	303	13172	39	145	109	25	212	8	836	standard

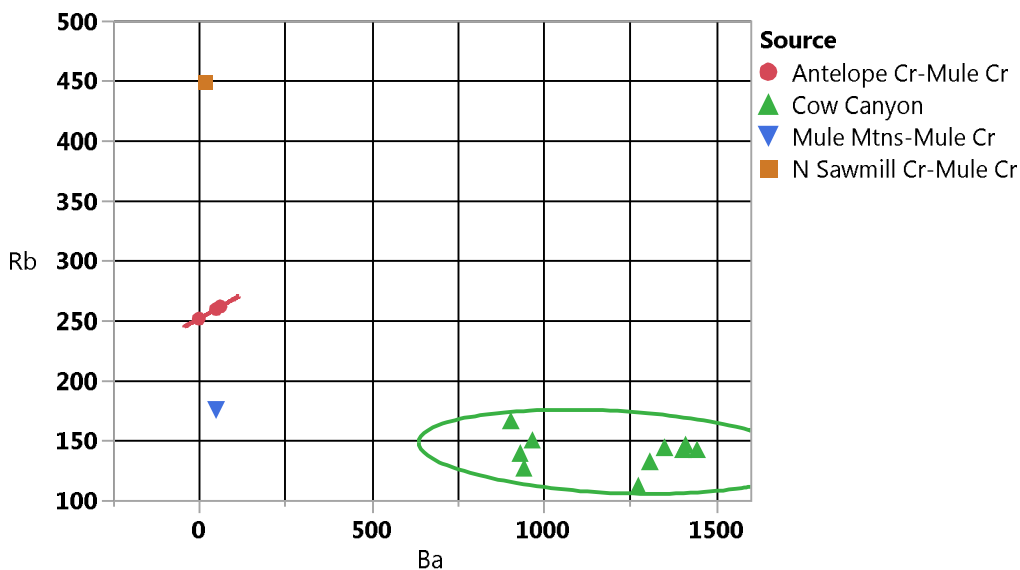


Figure 2. Ba versus Rb bivariate plot of the Sanchez Site obsidian artifacts and source assignments. Confidence ellipse at 95%.

*Source Provenance, Projectile Point Technology and Procurement Ranges*

While the source provenance of the obsidian artifacts is not necessarily useful in reconstructing procurement ranges in this case (see Shackley 1989, 1996), the style of the projectile points may be useful. Jane Sliva suggests that the two projectile points are Tularosa Corner-notched, a Late Archaic/Cienega Phase style most common in the uplands of the southeastern Colorado Plateau and the Tularosa Basin in south-central New Mexico (Sliva, personal communication, 8 August 2018; Sliva 2015:89-90, Fig. 2.77). This suggests that the Cow Canyon raw material could have been procured in the uplands where other points of this style have been recovered (see Figure 3 and cover image here).



Figure 3. Tularosa Corner-notched obsidian projectile points from Sanchez Site subsurface, both produced from Cow Canyon obsidian (see Sliva 2015:89-90 and Fig. 2.77).

### *Cow Canyon and Duncan Obsidian Sources*

During the 2016 UTSA field school a new obsidian source was discovered. This source, called the Duncan obsidian source just north of the town of Duncan, Arizona exhibits an elemental composition very similar to the Cow Canyon localities discussed above (Shackley 2018; Figure 4 here). Both appear to be members of the Mogollon-Datil Volcanic Province obsidian sources, and the similar composition is likely due to similar remelting of the underlying Precambrian granite basement (Elston 2008; Shackley et al. 2018). The two sources do vary in barium composition, so with XRF analyses barium needs to be acquired to discriminate these two sources, potentially relevant for archaeological problems (see Mills et al 2013).

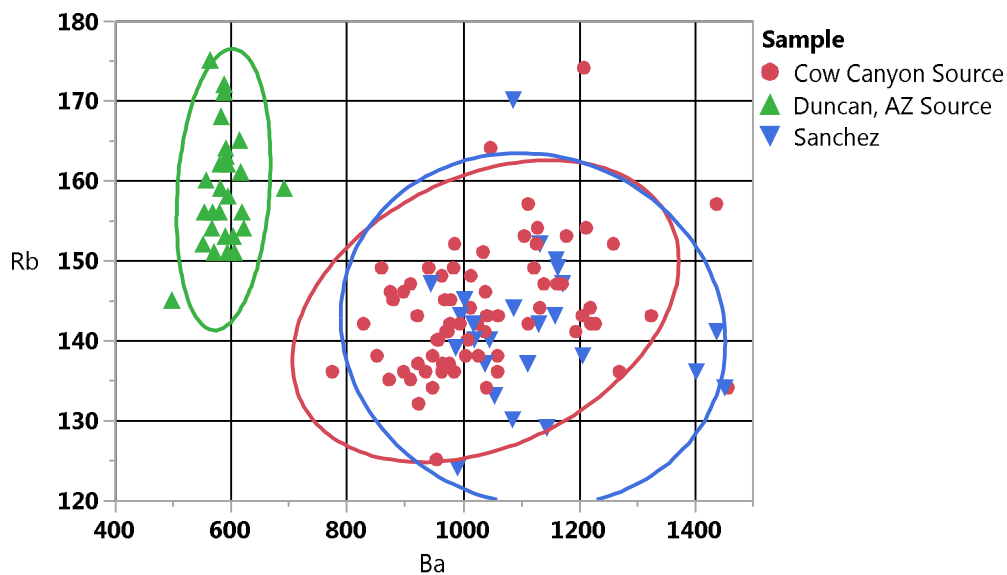


Figure 4. Ba versus Rb bivariate plot of Cow Canyon and Duncan source standards and the Cow Canyon assigned artifacts from the Sanchez Site. Confidence ellipses at 95%.

## REFERENCES CITED

- Davis, M.K., T.L. Jackson, M.S. Shackley, T. Teague, and J. Hampel  
2011 Factors Affecting the Energy-Dispersive X-Ray Fluorescence (EDXRF) Analysis of Archaeological Obsidian. In *X-Ray Fluorescence Spectrometry (XRF) in Geoarchaeology*, edited by M.S. Shackley, pp. 45-64. Springer, New York.
- Elston, W.E.  
2008 When Batholiths Exploded: the Mogollon-Datil Volcanic Field, Southwestern New Mexico. In *Geology of the Gila Wilderness-Silver City Area*, edited by G. Mack, J. Witcher, and V.W. Lueth, pp. 117-128. New Mexico Geological Society Guidebook, 59th Field Conference, Socorro, New Mexico.
- Govindaraju, K.  
1994 1994 Compilation of Working Values and Sample Description for 383 Geostandards. *Geostandards Newsletter* 18 (special issue).
- Hamilton, M.J., B. Buchanan, B.B. Huckell, V.T. Holliday, M.S. Shackley, and M. E. Hill  
2013 Clovis Paleoecology and Lithic Technology in the Central Rio Grande Rift Region, New Mexico. *American Antiquity* 78:248-265.
- Hampel, Joachim H.  
1984 Technical Considerations in X-ray Fluorescence Analysis of Obsidian. In *Obsidian Studies in the Great Basin*, edited by R.E. Hughes, pp. 21-25. Contributions of the University of California Archaeological Research Facility 45. Berkeley.
- Hildreth, W.  
1981 Gradients in Silicic Magma Chambers: Implications for Lithospheric Magmatism. *Journal of Geophysical Research* 86:10153-10192.
- Houser, B.B., D.H. Richter, and M. Shafiqullah  
1985 Geologic Map of the Safford Quadrangle, Graham County, Arizona. Miscellaneous Investigation Series, Map I-1617. U.S. Geological Survey, Denver.
- Hughes, Richard E., and Robert L. Smith  
1993 Archaeology, Geology, and Geochemistry in Obsidian Provenance Studies. *In Scale on Archaeological and Geoscientific Perspectives*, edited by J.K. Stein and A.R. Linse, pp. 79-91. Geological Society of America Special Paper 283.
- Kempton, K., G.R. Osburn, S. Kelley, M. Rampey, C. Ferguson, and J. Gardner  
2004 Geology of the Bear Springs Peak 7.5' Quadrangle, Sandoval County, New Mexico. Open File Geologic Map OF-GM 74 (Draft), New Mexico Bureau of Mineral Resources, Socorro.
- Mahood, Gail A., and James A. Stimac  
1990 Trace-Element Partitioning in Pantellerites and Trachytes. *Geochemica et Cosmochimica Acta* 54:2257-2276.

McCarthy, J.J., and F.H. Schamber

1981 Least-Squares Fit with Digital Filter: A Status Report. In *Energy Dispersive X-ray Spectrometry*, edited by K.F.J. Heinrich, D.E. Newbury, R.L. Myklebust, and C.E. Fiori, pp. 273-296. National Bureau of Standards Special Publication 604, Washington, D.C.

Mills, B.J., J.J. Clark, M.A. Peeples, W.R. Haas, Jr., J.M. Roberts, Jr., J.B. Hill, D.L. Huntley, L. Borck, R.L. Breiger, A. Clauset, and M.S. Shackley

2013 Transformation of Social Networks in the Late Pre-Hispanic US Southwest. *PNAS* 110:5785-5790.

Schamber, F.H.

1977 A Modification of the Linear Least-Squares Fitting Method which Provides Continuum Suppression. In *X-ray Fluorescence Analysis of Environmental Samples*, edited by T.G. Dzubay, pp. 241-257. Ann Arbor Science Publishers.

Shackley, M. Steven

1988 Sources of Archaeological Obsidian in the Southwest: An Archaeological, Petrological, and Geochemical Study. *American Antiquity* 53:752-772.

1989 *Early Hunter-Gatherer Procurement Ranges in the Southwest: Evidence from Obsidian Geochemistry and Lithic Technology*. Ph.D. dissertation, Department of Anthropology, Arizona State University, Tempe.

1992 The Upper Gila River Gravels as an Archaeological Obsidian Source Region: Implications for Models of Exchange and Interaction. *Geoarchaeology* 7(4):315-326

1995 Sources of Archaeological Obsidian in the Greater American Southwest: An Update and Quantitative Analysis. *American Antiquity* 60:531-551.

1996 Range and Mobility in the Early Hunter-Gatherer Southwest. In *Early Formative Adaptations in the Southern Southwest*, edited by Barbara Roth, pp. 5-16. Monographs in World Prehistory 25. Prehistory Press, Madison.

2005 *Obsidian: Geology and Archaeology in the North American Southwest*. University of Arizona Press, Tucson.

2007 Sources of Obsidian at the Murray Springs Clovis Site: A Semi-Quantitative X-Ray Fluorescence Analysis. In *Murray Springs: A Clovis Site with Multiple Activity Areas in the San Pedro Valley, Arizona*, edited by C.V. Haynes, Jr., and B.B. Huckell, pp. 250-254. Anthropological Papers of the University of Arizona 71, University of Arizona Press, Tucson.

2011 An Introduction to X-Ray Fluorescence (XRF) Analysis in Archaeology. In *X-Ray Fluorescence Spectrometry (XRF) in Geoarchaeology*, edited by M.S. Shackley, pp. 7-44. Springer, New York.

2018 A Newly Discovered Source of Archaeological Obsidian Near Duncan, Arizona and Its Compositional Relationship to the Cow Canyon Source, Eastern Arizona. *Kiva*, in review.

Shackley, M.S., L.E. Morgan, and D. Pyle

2018 Elemental, isotopic, and geochronological variability in Mogollon-Datil Volcanic Province archaeological obsidian, southwestern USA: solving issues of inter-source discrimination. *Geoarchaeology* 33:486-497.

Sliva, R. Jane

2015 *Projectile Points of the Early Agricultural Southwest: Typology, Migration, and Social Dynamics from the Sonoran Desert to the Colorado Plateau*. Archaeology Southwest, Tucson.